

Adsorption chiller in a combined heating and cooling system: simulation and optimization by neural networks

Jarosław KRZYWANSKI¹, Karol SZTEKLER², Marcin BUGAJ³, Wojciech KALAWA²,
 Karolina GRABOWSKA¹, Patryk Robert CHAJA^{4*}, Marcin SOSNOWSKI¹,
 Wojciech NOWAK², Łukasz MIKA², Sebastian BYKUĆ⁴

¹ Jan Długosz University in Czestochowa, Faculty of Science and Technology, ul. A. Krajowej 13/15, 42-200 Czestochowa, Poland

² AGH University of Science and Technology, Faculty of Energy and Fuels, ul. A. Mickiewicza 30, 30-059 Cracow, Poland

³ Warsaw University of Technology, Faculty of Power and Aeronautical Engineering, ul. Nowowiejska 24, 00-665 Warsaw, Poland

⁴ Institute of Fluid-Flow Machinery Polish Academy of Sciences, Department of Distributed Energy, ul. Fiszerza 14, 80-952 Gdansk, Poland

Abstract. Adsorption cooling and desalination technologies have recently received more attention. Adsorption chillers, using eco-friendly refrigerants, provide promising abilities for low-grade waste heat recovery and utilization, especially renewable and waste heat of the near ambient temperature. However, due to the low coefficient of performance (COP) and cooling capacity (CC) of the chillers, they have not been widely commercialized. Although operating in combined heating and cooling (HC) systems, adsorption chillers allow more efficient conversion and management of low-grade sources of thermal energy, their operation is still not sufficiently recognized, and the improvement of their performance is still a challenging task. The paper introduces an artificial intelligence (AI) approach for the optimization study of a two-bed adsorption chiller operating in an existing combined HC system, driven by low-temperature heat from cogeneration. Artificial neural networks are employed to develop a model that allows estimating the behavior of the chiller. Two crucial energy efficiency and performance indicators of the adsorption chiller, i.e., CC and the COP, are examined during the study for different operating sceneries and a wide range of operating conditions. Thus this work provides useful guidance for the operating conditions of the adsorption chiller integrated into the HC system. For the considered range of input parameters, the highest CC and COP are equal to 12.7 and 0.65 kW, respectively. The developed model, based on the neurocomputing approach, constitutes an easy-to-use and powerful optimization tool for the adsorption chiller operating in the complex HC system.

Key words: adsorption heat pumps; polygeneration; cooling capacity; low-grade thermal energy; artificial neural networks; soft computing.

Nomenclature

A_c	collector area, m ²	NN	Neural Network
ACANN	Adsorption Chiller by Artificial Neural Networks model	VH	Volume flow rate of hot water, dm ³ /min
AdC	Adsorption Chiller	VL	Volume flow rate of ice-water, dm ³ /min
AI	Artificial Intelligence	VM	Volume flow rate of recooling water, dm ³ /min
ANFIS	Adaptive Neuro-Fuzzy Inference System	T	Temperature, K
ANN	Artificial Neural Networks	THin	Inlet temperature of hot water, K
BTES	Borehole Thermal Energy Storage	THout	Outlet temperature of hot water, K
CC	Cooling Capacity, kW	TLin	Inlet temperature of ice-water, K
COP	Coefficient of Performance, –	TLout	Outlet temperature of ice-water, K
HP	Heating Power, kW	TMin	Inlet temperature of recooling water, K
HTBT	High Temperature Buffer Tank, K	TTES	Tank Thermal Energy Storage
HTHP	High Temperature Heat Pump, K		
LTBT	Low Temperature Buffer Tank (Ice Water), K		
ML	Machine Learning		
MTBT	Medium Temperature Buffer Tank, K		

*e-mail: patryk.chaja@imp.gda.pl

Manuscript submitted 2020-07-31, revised 2021-03-05, initially accepted for publication 2021-03-05, published in June 2021

1. Introduction

Waste heat recovery is nowadays a common practice as such heat source is available in large quantities at different temperature levels worldwide, especially with low parameters generated as a by-product [1, 2]. According to Rezaie and Rosen, the efficient and intelligent use of energy waste, including low-temperature waste heat, belongs to the critical actions to address energy and environmental challenges [3]. Roskilly and Al-Nimr remarked that improving energy efficiency and reducing both

energy demand and greenhouse gas emissions are significant challenges nowadays [4]. The ability to use waste heat, but also renewable and recycled heat from low-temperature sources, is also set into the concept of the 4th Generation District Heating (4GDH), defined by Lund in [5] and also mentioned in [6].

Adsorption cooling technology is one of the most effective ways of cooling and potable water production [7–11]. A simple configuration without moving parts, application of eco-friendly refrigerants, the ability to low-grade heat recovery and utilization, especially renewable and waste heat of the near ambient temperature, including sewage water, underground resources, solar heat, constitute the main advantages of adsorption chillers [12–14]. On the other hand, unfavorable heat exchange conditions in the porous sorbent bed and the resulting low coefficients of performance (COP) are their main disadvantages, resulting in numerous optimization works of these appliances [15–19].

A thermodynamic model of a three-bed adsorption chiller with a cooling capacity equal to 90 kW is shown in [7]. Optimization of adsorption dynamics in adsorbent beds of loose grains was performed in [20]. The dynamic optimization of adsorptive chillers was demonstrated in [21]. Genetic algorithms and neural networks were introduced for a cooling capacity (CC) optimization study of a tri-bed, twin-evaporator adsorption chiller in [2]. A nonlinear model-predictive-control for adsorption coolers was discussed in [22]. A detailed numerical model of a two-bed adsorption chiller developed to examine the effects of operating and geometrical parameters on its overall performance is shown in [23]. A neuro-adaptive fuzzy-inference system (ANFIS) approach, to optimize CC of a re-heat, two-stage adsorption chiller in a wide range of both design and operating parameters, was developed in [24]. A dimensional analysis to optimize adsorption performance for desired operating conditions including adsorbent–vapor pair, adsorption duration, operational pressure, intercrystalline porosity, adsorbent crystal size, and intercrystalline vapor diffusivity – was carried out in [25]. A reallocation of adsorption/desorption cycle times to optimize the performance of adsorption chillers is discussed in [26]. A comparison of different kinds of heat recovery systems applied in an adsorption refrigeration unit is shown in [27].

A state-of-the-art overview of modeling techniques of adsorption cooling systems is demonstrated in [28]. The authors underlined that further extensive research work is necessary to optimize the performance of adsorption chillers, and more advanced models need to be developed.

Promising approaches allowing to address contemporary problems is the AI methods, including artificial neural networks (ANN) [29–31]. The ANNs have been widely used in different areas, including modeling and optimization [32–35]. Different kinds of neural networks can be distinguished, including e.g., deep and shallow neural networks, function fitting neural networks, generalized regression neural networks, cascade-forward neural networks, feed-forward neural networks, RBF, and Kohonen networks [36–38]. The ensemble of many neural predictors are also interesting and promising alternatives [39].

Deep learning versus classical neural approach to mammogram recognition was compared in [40]. A comprehensive com-

parative study of different state-of-art machine learning methods used for breast cancer diagnosis was conducted in [41]. A fast multispectral deep fusion network was developed in [42]. The use of convolutional neural network AlexNet for the detection of driver fatigue symptoms was depicted in [43]. The ANN-based approach was also implemented for computational gait analysis for post-stroke rehabilitation purposes [44] and for modeling and the optimization of the effect of nozzle type, spray pressure, driving speed, and spray angle on spray coverage [45]. Decoupling control for permanent magnet in-wheel motor using internal model control based on the back-propagation neural network inverse system was shown in [46]. An assessment of wind energy resources using artificial neural networks was performed in [47].

This paper deals with a neurocomputing approach in modeling a two-bed adsorption chiller (AdC) incorporated into an existing, combined heating and cooling (HC) system, using waste heat as low-grade thermal energy from cogeneration.

The developed Adsorption Chiller by Artificial Neural Networks (ACANN) model is based on an artificial neural network (ANN) approach and allows successfully estimating two crucial energy efficiency and performance indicators of the adsorption chiller, i.e., cooling capacity (CC) and coefficient of performance (COP) [23] for a wide range of operating parameters. The training samples, necessary to develop the model, are taken from experiments similar to the methods described in [2, 48].

The proposed approach can be treated as an alternative technique of data handling, considering the complexity of numerical and analytical methods and high costs of empirical experiments [49–54].

2. The research object and methods

Experimental research related to the integration of an adsorption chiller with a high-temperature CO₂ heat pump was carried out on an innovative installation presented in Fig. 1.

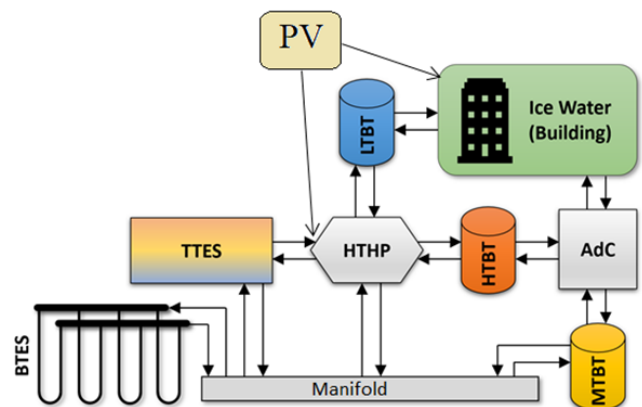


Fig. 1. Schematic diagram of the Combined Hybrid Heating and Cooling System: HTBT – High-Temperature Buffer Tank, AdC – Adsorption Chiller, MTBT – Medium Temperature Buffer Tank, LTBT – Low-Temperature Buffer Tank (ice water), HTHP – High-Temperature Heat Pump, BTES – Borehole Thermal Energy Storage, TTES – Tank Thermal Energy Storage, PV – photo-voltaic module

The adsorption chiller produces environmentally friendly cooling energy from waste heat using water as the refrigerant and silica gel as the adsorbent. The most important parts of the experimental installation are a high-temperature buffer tank (HTBT), adsorption chiller (AdC), medium temperature buffer tank (MTBT), high-temperature heat pump (HTHP), borehole thermal energy storage (BTES), and tank thermal energy storage (TTES). In the experimental installation, a high-temperature heat pump (HTHP) of CO₂ produced by MAYEKAWA (HWW-2HTC) was used as the desorption heat source process. The device can recover waste heat stored in TTES, gain energy from the boreholes and supply ice water, as the overall system's main task is to provide cooling for the building. Significant differences in temperature level compared to standard heat pumps result from the fact that the CO₂ works in supercritical conditions. The PV array generates electrical energy, which causes that the supply of "free" electricity for the HTHP drive is coherent with the demand for cold, which reduces the cost of cooling the building. Usually, the high-grade heat from the HTHP would be disposed of, but thanks to the AdC, it is partially recovered, and the waste heat temperature is decreased.

The HTHP supplies ice water and simultaneously hot water to regenerate AdC's adsorption bed. The produced ice water in the AdC is directly used to chill the building infrastructure, or when the building is sufficiently cold, it is stored in LTBT. The cooling water circuit of the AdC is connected to the MTBT tank, where the heat carrier temperature is controlled by the use of a loop connected with BTES via a manifold. The whole system is assembled into one unit to provide controlled conditions of the installation.

Regarding the considered AdC, three circuits can be distinguished: hot water circuit (driving circuit), recooling circuit, and ice water circuit. The hot water circuit supplies the thermal energy driving the adsorption chiller. The recooling circuit moves the heat from the adsorption bed, cooling it during the sorption stage. Finally, the ice water circuit removes heat from the object being cooled (the building) as the AdC is designated for using the waste low-temperature heat of industrial systems.

In the experiment, temperature and flow measurements data was collected every second. For measurements of temperature hot water, chilled water and cooling were used, the thermistors Pt100 Ω ($\pm 0.2^\circ\text{C}$) PT-1000 Ω (range from -80 to 150°C), $\pm 0.2^\circ\text{C}$. Pressure sensors range 0–99 kPa, precision 0,5% FS, 4–20 mA, were used to measure the pressures in condenser, evaporator, and beds. Electromagnetic flow meters 0,5% FS, 4–20 mA were used to measure the flow rate of the heating water, cooling water and chilled water.

A neurocomputing approach is applied to develop the ACANN model. The method consists of the use of artificial neural networks (ANN) as one of the most potent techniques of machine learning (ML) and artificial intelligence (AI). The ANNs can reproduce models from training samples and extract knowledge from the data to determine complex relationships between them [2, 30, 39, 40]. The best generalization abilities an ANN possesses when the ANN's mapping represents the underlying systematic aspects of the data, i.e., complex relationships

between input and output variables, rather than capturing specific details, including noise contribution of the particular data set [48, 55].

An artificial neural network constitutes a biologically inspired computational model with neurons grouped into layers [48, 55–57]. This soft computing method can generalize acquired knowledge [58]; thus, the discussed application deals with approximation issues for optimal CC and COP performance parameters.

Neural Designer software is employed to reproduce the adsorption chiller operation from measured data [55]. It is a data machine learning platform for advanced data analysis using artificial neural networks. It allows implementing deep NN architectures with an arbitrary number of perceptron layers for very complex data sets, where deeper architectures of three, four, or more perceptron layers may be required [55]. ANNs have universal approximation properties, enabling approximation of any function in any dimension [55]. Since most neural networks, even biological neural networks, exhibit layered structures, the ANN consists of a group of interconnected neurons arranged into layers [29, 59].

Three different subsets: training, selection, and testing, make the total number of data employed while performing the model, allowing to avoid the network's ability to memorize solutions and to make the network generalize the knowledge of the system.

Training instances are the data for developing various ANN models of different architectures and comparing their performance. Selection instances are applied to select the model with the best generalization abilities. Finally, to validate the functioning model and test its capabilities, testing instances are necessary. Thus the general design procedure covers the following main steps:

- loading and preprocessing the data including splitting them into training, selection, and testing sets),
- defining the NN structure, e.g., the number of layers and neurons in each layer, activation function),
- training, testing, and deploying the model [55].

The assumed parameters used to develop the ACANN model are described in the next sections.

3. Results and discussion

3.1. Application and validation of the ACANN model. The operational data acquired during the measurement campaign allowed us to develop and validate the ACANN model. A neural network was trained based on a training data set consisting of input-target training samples [2, 55]. Input variables represent physical measurements of water temperatures and volume flow rates during AdC operation. The following values: inlet volume flow rate and temperatures of ice water (VL, TLin), recooling water (VM, TMin), and hot water (VH, THin) are assumed as input parameters. The data are presented in Table 1.

The above range of the input parameters was defined, considering the operating conditions of the considered combined heating and cooling system.

Table 1
The input parameters variables used in the study

	Minimum	Maximum
TLin, K	283	293
TMin, K	288	298
THin, K	331	358
VL, dm ³ /min	1	20
VM, dm ³ /min	70	80
VH, dm ³ /min	13	30

A total number of 3962 instances are employed to develop the ACANN model. The random data splitting method with basic training, selection, and testing instance ratios of 0.60, 0.20 and 0.20, respectively, generated a training data subset, with a total of 2378 samples and the selection and testing subsets with 792 instances, each. A wide range of operating parameters is considered in the study (Table 1).

The ice-water (TLout) and hot water (THout) outlet temperatures constitute the ACANN model’s outputs. They allowed to easily derive the two fundamental energy efficiency and performance indicators of the adsorption chiller, i.e., cooling capacity (CC) and coefficient of performance (COP) [13].

Since an ANN operation depends on topology, including the number of layers and neurons in each layer, different ANN architectures were tested during the study [2, 57]. The best selection method allowed us to obtain a complex level model, which is the most appropriate to produce an adequate fit of the data. To avoid the two frequent problems in the design of NNs, called underfitting and overfitting, and to achieve the best generalization capabilities, the model’s complexity should be appropriate to the problem studied. Underfitting and overfitting are the effects of a selection error increase caused by too simple or too complex models, respectively.

Two powerful functionalities, i.e., order selection and inputs selection algorithms, are implemented into the Neural Designer platform. These methods help to find an optimal ANN with the best generalization properties, i.e., with the lowest error on the selection data. In other words, these innovative algorithms allow the automation of the model selection procedure, and finding a neural network topology that minimizes the error on new data, improving generalization performance [55].

The first algorithm, called the order selection task, is responsible for finding the optimal, hidden perceptron number. During this task, the neural network order is modified to obtain the optimum selection loss as the selection error is a measure of the ANN’s ability to predict the results for new cases, unseen before by the network [55]. For this study, the incremental order method was employed, as it is the most straightforward order selection algorithm.

The inputs selection algorithm selects a subset of inputs more influential on a particular physical process, allowing to find the optimal subset of inputs for the best loss of the model [55].

The genetic algorithm was applied in the input selection procedure as it is the most advanced instance of the model selection

algorithms, based on the mechanisms of natural genetics and biological evolution, implementing selection, crossover, and mutation operators [55, 59].

The Hyperbolic Tangent activation function is selected for hidden and output neurons as it is one of the most widely used transfer functions when constructing neural networks [2, 55].

Mean squared error served as the error estimation method in loss function expression during the training stage by the quasi-Newton method algorithm. The following plot shows the losses in each iteration (Fig. 2).

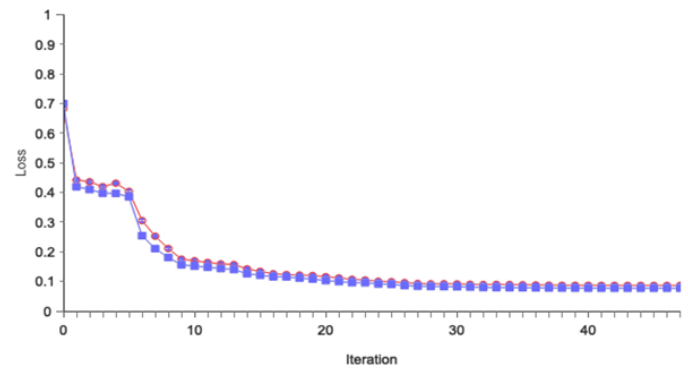


Fig. 2. The Quasi-Newton Losses Method History (the blue line expresses the training loss, whereas the red one corresponds to selection loss)

The trends in Fig. 2, show the good ability of the considered ANN to train the process. Thus the training process was smooth and effective. The initial and final values of training losses are 0.700 and 0.0771, respectively, while the initial and final values of the selection losses are 0.6825 and 0.0865, respectively.

The optimal neural network, after the model selection task [55], turned out to be [6–112] with two hidden layers composed of one neuron in each layer, six inputs, and two output neurons. The final testing error, after the model selection task, corresponding to the final network architecture, is equal to 0.0869.

Figure 3 shows a graphic representation of the final network topology. The model also contains a scaling layer and an unscaling output layer. The yellow circles represent scaling neurons, the blue ones are perceptron neurons, and the red circles correspond to unscaling neurons. The goal of the scaling procedure is to keep all inputs within the range of 0–1. Thus, the scaled outputs from a neural network should be unscaled to produce the original units [55, 56, 60, 61].

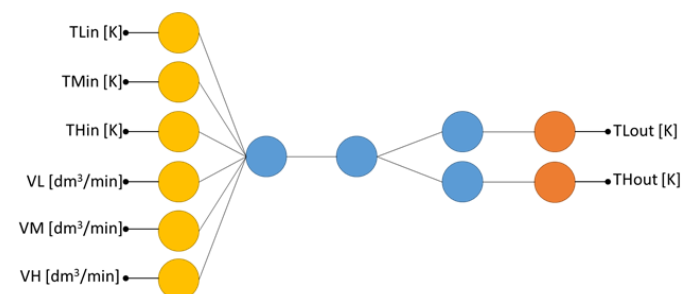


Fig. 3. The Architecture of the ACANN model

It is worth mentioning that this three-layered neural network, including two hidden oneneuronal layers and one two-neuronal output layer, can be reproduced as the industrial scale AdC operating in the combined heating and cooling system. This architecture meets the main requirements for neural networks, according to which at least two neuronal layers are mandatory to be capable of describing complex, nonlinear processes [29, 62].

Finally, during the test stage, the comparison between predicted outputs and targets from the independent data set, called “testing instances” is carried out [55].

A linear regression analysis between the scaled neural network outputs and the corresponding targets for an independent testing subset is a standard testing method. Figure 4 shows the linear regression chart for the outputs TLout (a) and THout (b).

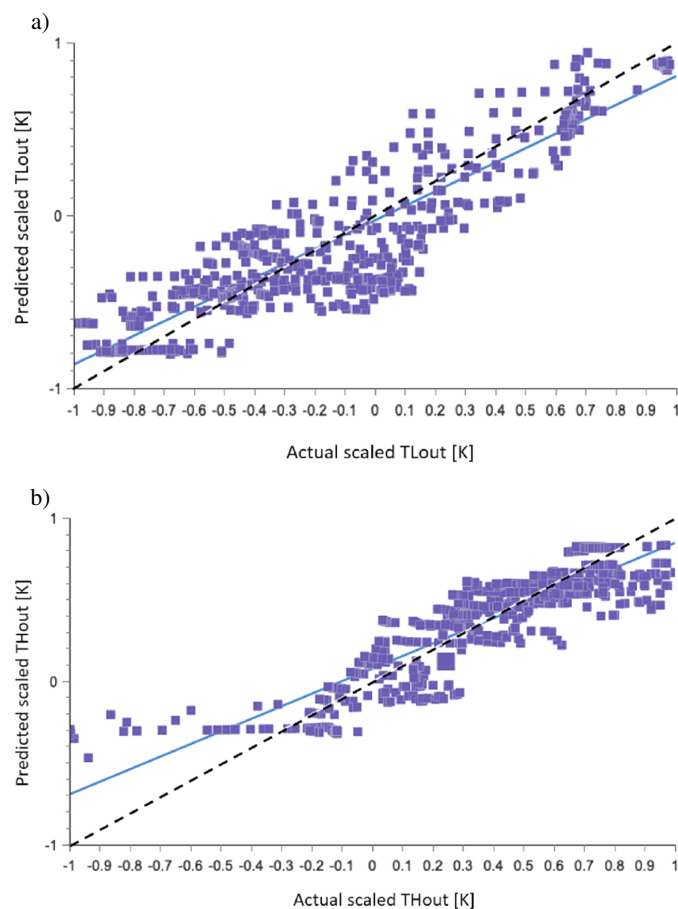


Fig. 4. Scatter Plots for Outputs: a) TLout and b) THout (the blue and dashed lines indicate the best and perfect fits, respectively)

Table 2 demonstrates the three parameters resulting from the linear regression, i.e., y-intercept, the slope of the best linear regression for targets and scaled outputs, and the correlation coefficient between them.

Since the y-intercept and the correlation coefficient are close to 0 and 1, respectively, the model’s outputs are close to targets.

Thus, also considering the final loss values, the developed ACANN’s model has good accuracy and is ready to be used for making predictions and analyzing the influence of input variables on the AdC performance [55].

Table 2
Parameters of Linear Regression Analysis

	TLout	THout
Intercept	-0.0283	0.0784
Slope	0.837	0.771
Correlation	0.914	0.889

3.2. Influence of operating parameters on the performance of the AdC.

An interesting issue is to see how a single input influences the performance of the adsorption chiller. Such an approach constitutes a cut of the neural network model along some input direction and through a reference point [55]. A reference point for further calculations that correspond to the values usually found in the tested unit are listed in the captions of the figures. However, the dependencies between input parameters, i.e., TLin, TMin, THin, VL, VM, and VH, ought to be also considered taking into account complex thermal and flow processes that occur in the AdC operating in the combined heating and cooling system.

It is essential to underline that the behavior of the AdC, incorporated into the hybrid heating and cooling system, differs from the stand-alone mode, as each part of the loop influences one another, and this also stands for one of the main contributions of the paper.

3.2.1. Effect of the ice water inlet temperature and volume flow rates.

The effect of the ice water inlet TLin temperature on the outlet ice and hot water temperatures TLout and THout, respectively, are shown in Fig. 5. The increase in TLin leads to an increase in its outlet temperature. Such behavior is the result of two mechanisms [63]. The increase in inlet temperature causes the rise in heat flux between the ice water and the refrigerant in the evaporator, especially at the inlet area of the evaporator’s tubes. That is why the tubes pass arrangement in the evaporator is a crucial factor influencing the entire system performance [59, 64, 65]. However, the increase in the heat transfer

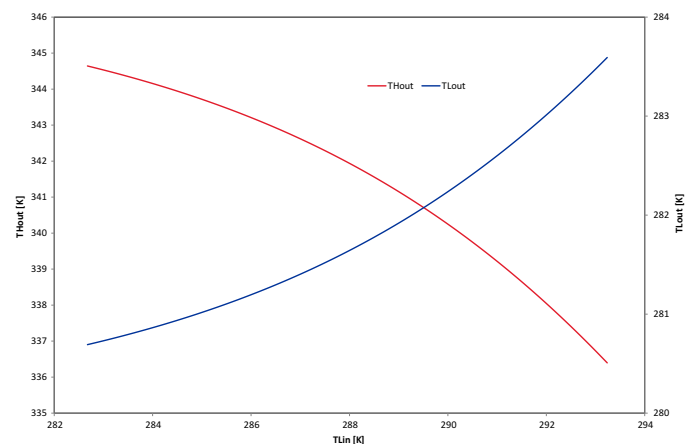


Fig. 5. Effect of the ice water inlet temperature on the outlet temperatures of the ice and hot water (TLin = 283 K–293 K, TMin = 298 K, THin = 353 K, VL = 20 dm³/min, VM = 75 dm³/min, VH = 15 dm³/min)

rate is limited as the water vaporization in the evaporator cannot transfer out the entire increased energy supply in the inflowing warmer water stream, resulting in a higher outlet temperature TL out (Fig. 5).

On the other hand, the increased heat flux in the evaporator promotes higher vapor production. The higher amount of adsorbed water vapor allows for the rise in the heat amount expelled in the desorption stage, leading to the increase in heating power and the decrease in the hot water output temperature (Fig. 5).

Figure 6 shows the effect of ice water inlet temperature TLin on the CC and COP. The increase in TLin leads to an increase in both CC and COP. However, for TLin higher than 291 K, at which the COP attains the maximum, the COP slightly decreases due to the high heating power generated in the adsorption bed during the desorption stage. Hence, taking into account the results from Fig. 6, the value 291 K should be considered as the optimum one as the COP reaches its maximum.

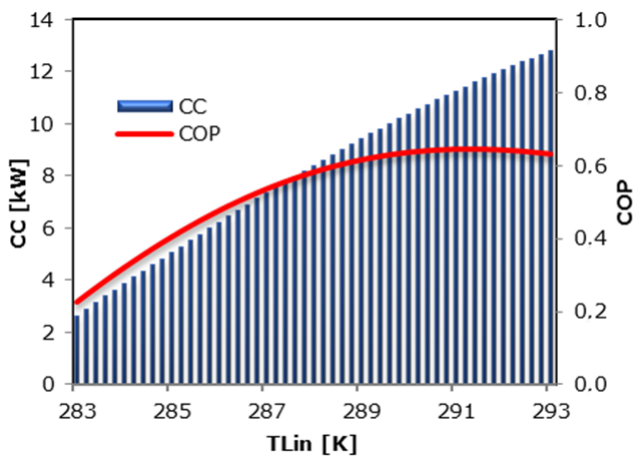


Fig. 6. Effect of the ice water, inlet temperature on CC, and COP of the adsorption chiller (TLin = 283 K–293 K, TMin = 298 K, THin = 353 K, VL = 20 dm³/min, VM = 75 dm³/min, VH = 15 dm³/min)

The influence of the ice water volume flow rate VL on TLout, THout, CC, and COP is shown in Figs. 7 and 8. The increase in

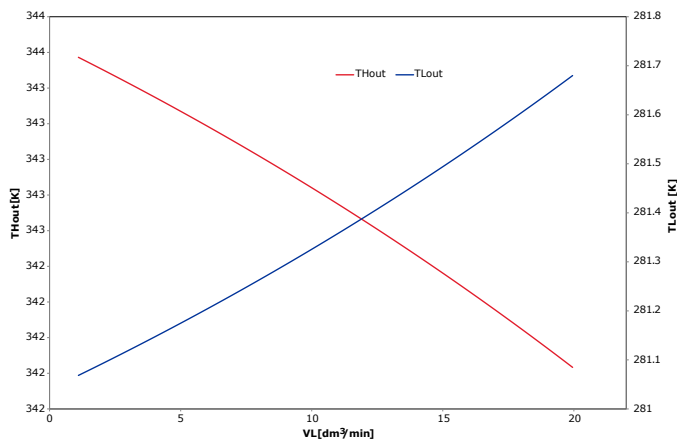


Fig. 7. Effect of the ice water volume flow rates on the outlet temperatures of the ice and hot water (TLin = 288 K, TMin = 298 K, THin = 353 K, VL = 1–20 dm³/min, VM = 75 dm³/min, VH = 15 dm³/min)

the VL leads to a slight increase in output temperature TLout (Fig. 7). Since the inlet ice water temperature is equal to 288 K, the heat supplied together with the inflowing water stream cannot be carried out by a limited increase in the heat transfer rate for higher water velocities (Fig. 11).

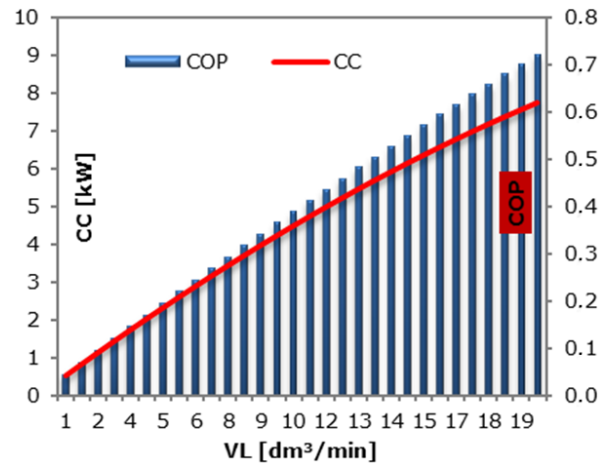


Fig. 8. Effect of the ice water volume flow rates on CC and COP of the AdC (TLin = 288 K, TMin = 298 K, THin = 353 K, VL = 1–20 dm³/min, VM = 75 dm³/min, VH = 15 dm³/min)

However, this increased heat transfer rate intensifies water vapor production, which, accumulated on the inner surface of the silica gel, expelled together with the heat from the bed during desorption, leads to a slight decrease in THout. The above-described effects are expressed in increased CC and COP values, as shown in Fig. 8.

3.2.2. Effect of the recooling water inlet temperature and volume flow rates.

Figure 9 shows the influence of recooling water inlet temperature TMin on temperatures TLout and THout. The increase in TMin simulates the heat recovery system of the AdC, which is one of the most important methods of improving the performance of the adsorption cooling systems.

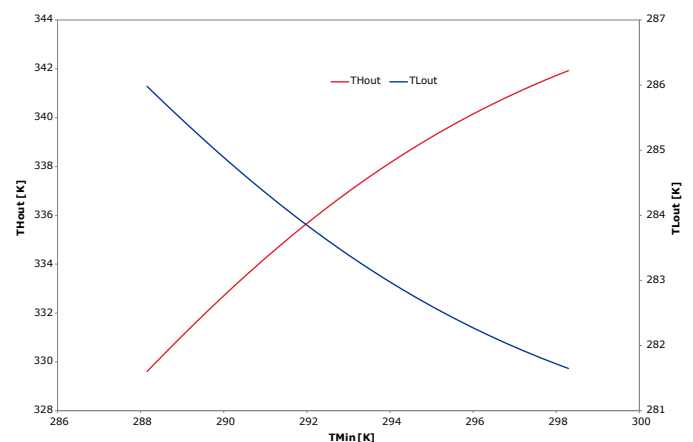


Fig. 9. Effect of the recooling water, inlet temperature on the outlet temperatures of the ice, and hot water (TLin = 288 K, TMin = 288 K–298 K, THin = 353 K, VL = 20 dm³/min, VM = 75 dm³/min, VH = 15 dm³/min)

In this technique, a part of the heat released during bed cooling can be partly used to heat the other bed instead of being conventionally discharged into the environment as waste energy [18]. In other words, when a two-bed adsorption chiller employs the heat recovery system, the heat generation in the first adsorber during the phase of desorption is used to heat the second one before desorption. In the next phase, the two beds will switch the role of heating and cooling [18].

The considered AdC also uses the heat recovery system. The return line of the adsorber, which is desorbed immediately following the adsorption, is routed to the recooling circuit. Such operation leads to an increase in T_{Min} , according to Fig. 9, and allows better preparation of the adsorption bed to the consecutive desorption stage, resulting in a decrease in the ice water outlet temperature T_{Lout} .

On the other hand, the increase in T_{Min} causes a decrease in temperature difference between the recooling and hot water, leading to an increase in the hot water outlet temperature T_{Hout} , observed in Fig. 9 [66].

The obtained results are in coincidence with the observed effects of T_{Min} on CC and COP, depicted in Fig. 10.

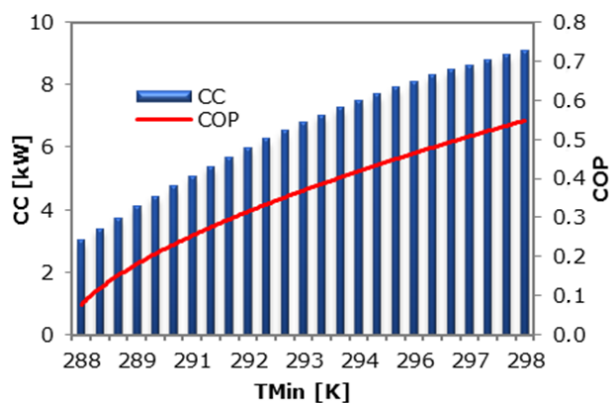


Fig. 10. Effect of the recooling water inlet temperature on CC and COP of the adsorption chiller ($T_{Lin} = 288$ K, $T_{Min} = 288$ K–298 K, $T_{Hin} = 353$ K, $V_L = 20$ dm³/min, $V_M = 75$ dm³/min, $V_H = 15$ dm³/min).

The increase in the recooling water temperature leads to an increase in these two energy efficiency and performance indicators of the adsorption chiller, i.e., CC and COP, as the recovery system improves the ADS performance [18].

Lower ice water output temperatures (Fig. 9) favor lower pressures in the evaporator, allowing an increase in the amount of vapor produced and higher cooling capacity of the adsorption chiller [67]. Furthermore, due to an increase in T_{Hout} , the heating power HP of the AdC decreases. The simultaneous increase in CC and a decrease in HP cause a further increase in COP of the system, according to Fig. 10 [13].

The effects of the volume flow rates of recooling water VM on T_{Lout} , T_{Hout} , CC, and COP are shown in Figs. 11 and 12.

The increase in the recooling water volume flow rates slightly influences the output temperatures, causing a small rise and a decrease in T_{Hout} and T_{Lout} , respectively, by ca. 1–2 K. The observed changes are results of slight heat transfer improve-

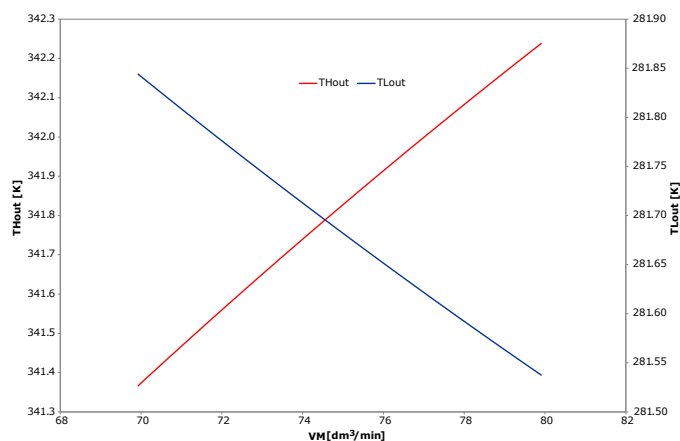


Fig. 11. Effect of the recooling water volume flow rates on the ice and hot water outlet temperatures ($T_{Lin} = 288$ K, $T_{Min} = 298$ K, $T_{Hin} = 353$ K, $V_L = 20$ dm³/min, $V_M = 70$ –80 dm³/min, $V_H = 15$ dm³/min)

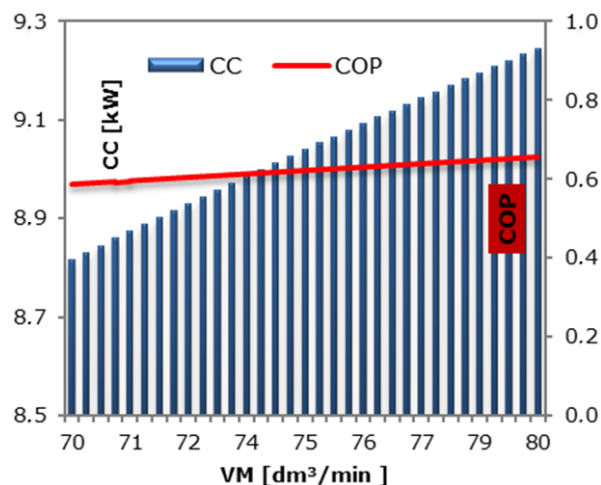


Fig. 12. Effect of the recooling water volume flow rates on CC and COP of the AdC ($T_{Lin} = 288$ K, $T_{Min} = 298$ K, $T_{Hin} = 353$ K, $V_L = 20$ dm³/min, $V_M = 70$ –80 dm³/min, $V_H = 15$ dm³/min)

ment in the heat exchanger of the adsorption bed for higher fluid velocities. Such conditions lead to an increase in CC [68].

However, the increase in VM means a decrease in temperature difference between the recooling and hot water due to the recovery system applied in the considered AdC aggregate, discussed in the previous section. Thus the increase in the recooling water volume flow rates leads to lowering the heating power HP of the chiller. The simultaneous increase in CC and a decrease in HP cause an increase in COP reported in Fig. 12.

It is also worth noting that, based on the training sample, the developed ACANN model accurately identified the beneficial effects of the heat recovery system, improving the waste thermal energy management in the chiller.

That is why the AI models, which are capable of reproducing a process or an object behavior without specific knowledge, are sometimes deemed to be tools that can overcome the shortcomings of the programmed computing approach and the experimental procedures [2, 48, 59].

3.2.3. Effect of hot water inlet temperature and volume flow rates.

Figure 13 shows the effect of hot water inlet temperature TH_{in} on the outputs TL_{out} and TH_{out} . As the TH_{in} increases, the ice water output temperature from the evaporator TL_{out} slightly decreases. Higher hot water temperatures cause an increase in bed temperature. These conditions allow better preparing the bed for the adsorption phase by expelling to the condenser more refrigerant, previously accumulated on the inner surface of the silica gel. Such a well-prepared adsorption bed has a higher capacity to absorb more water vapor and favors adsorption processed, leading to a decrease in TL_{out} [63].

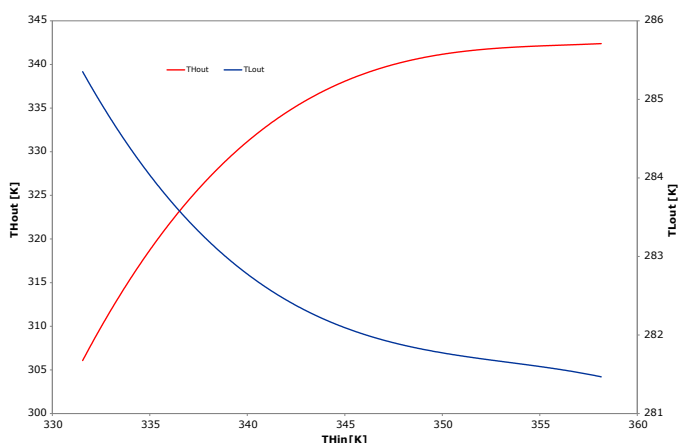


Fig. 13. Effect of the hot water inlet temperature on the outlet temperatures of the ice and hot water ($TL_{in} = 288$ K, $TM_{in} = 298$ K, $TH_{in} = 331$ K–358 K, $VL = 20$ dm³/min, $VM = 75$ dm³/min, $VH = 15$ dm³/min)

However, since not all of the heat input, supplied with hot water, can be carried out in the vapor steam expelled to the condenser, the increase in hot water inlet temperature TH_{in} leads to the increase in its output temperature TH_{out} (Fig. 13).

The effects of TH_{in} on CC and COP are the results of two opposing mechanisms shown in Fig. 14. The cooling capacity of the adsorption chiller increases with the increase in TH_{in} .

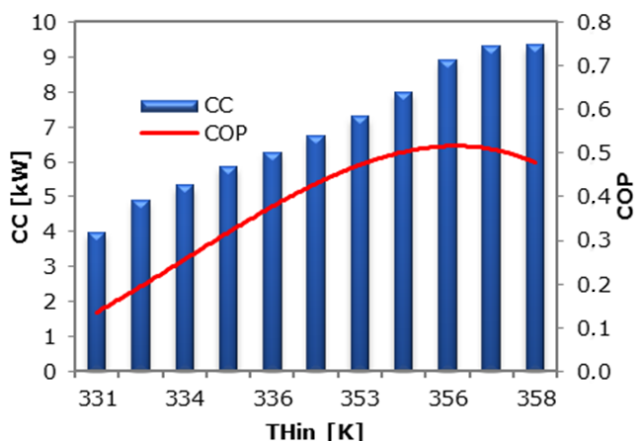


Fig. 14. Effect of the hot water, inlet temperature on CC, and COP of the AdC ($TL_{in} = 288$ K, $TM_{in} = 298$ K, $TH_{in} = 331$ K–358 K, $VL = 20$ dm³/min, $VM = 75$ dm³/min, $VH = 15$ dm³/min)

Since the bed regeneration process is more complete, due to better thermal conditions corresponding to higher hot water inlet temperatures TH_{in} , the refrigeration circulation increases with the increase in the amount of desorbed refrigerant and the equilibrium uptake of water vapor is higher for the thorough regenerated bed. Such conditions improve the cooling capacity CC [66,69–71]. On the other hand, as CC improves, the heating power HP of the AdC also increases, leading for TH_{in} higher than 356 K to the decrease in COP (Fig. 14).

Figures 15 and 16 show the effects of the hot water volume flow rate on the TL_{out} , TH_{out} , CC, and COP of the adsorption chiller. The increase in VH slightly improves heat transfer in the tubes of the heat exchanger.

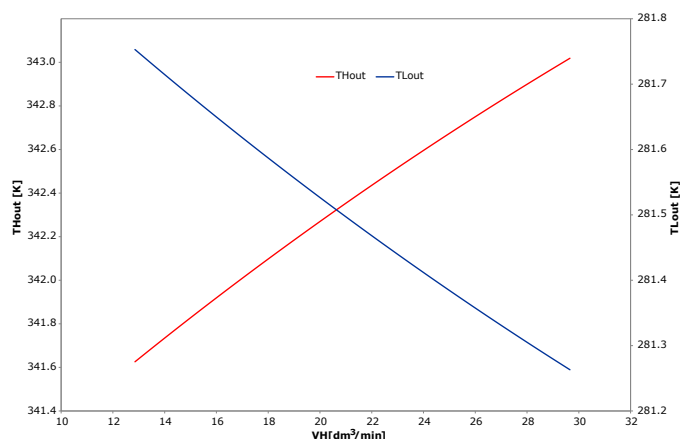


Fig. 15. Effect of the hot water volume flow rates VH on the outlet temperatures of the ice and hot water ($TL_{in} = 288$ K, $TM_{in} = 298$ K, $TH_{in} = 353$ K, $VL = 20$ dm³/min, $VM = 75$ dm³/min, $VH = 13$ –30 dm³/min)

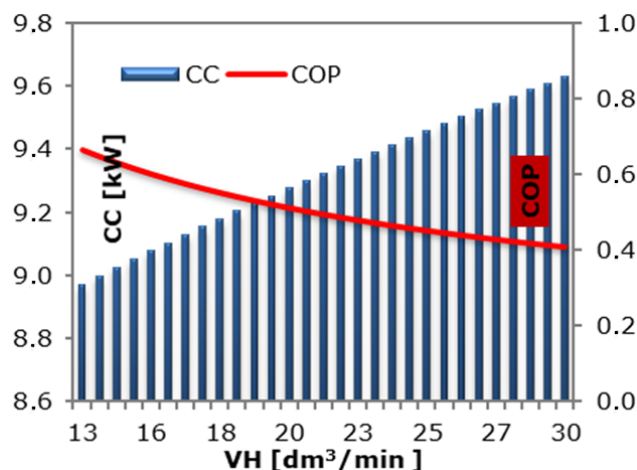


Fig. 16. Effect of the hot water volume flow rates on CC and COP of the adsorption chiller ($TL_{in} = 288$ K, $TM_{in} = 298$ K, $TH_{in} = 353$ K, $VL = 20$ dm³/min, $VM = 75$ dm³/min, $VH = 13$ –30 dm³/min)

This favors the desorption process, allowing to increase the vapor uptake during the adsorption stages. Such conditions cause a slight decrease in ice water output temperatures TL_{out} , increasing CC.

However, as the increased heat supply, corresponding to higher VH and better heat transfer conditions cannot be entirely consumed by the desorption processes, the increase in the hot water volume flow rate VH cause a slight increase in THout.













The increased hot water volume flow rates mean higher Reynolds numbers and an increase in heat transfer rates inside the tubes of a heat exchanger in the adsorption, causing the increase in heating power HP of the AdC. As a result, the coefficient of performance decreases with VH (Fig. 16).

3.2.4. The best strategy in energy conversion management.

On the basis of the observed trends in CC and COP, for the considered range of input parameters, the effects of inputs can be summarized as were shown in Table 3.

Table 3

Effect of an increase in input parameters on CC and COP of the AdC

Parameter (horizontal axis)	CC (vertical axis)	COP (vertical axis)
Ice water inlet temperature, T _{Lin} , K		
Cooling water inlet temperature, T _{Min} , K		
Heating water inlet temperature, T _{Hin} , K		
Ice water volume flow rate, VL, dm ³ /min		
Recooling water volume flow rate, VM, dm ³ /min		
Hot water volume flow rate, VH, dm ³ /min		

The cooling capacity CC of the AdC, incorporated into the considered combined heating and cooling system, can be intensified by the increase in all inputs.

The highest CC, equal to 12.7 kW can be reached for T_{Lin} = 293 K, T_{Min} = 298 K, T_{Hin} = 353 K, VL = 20 dm³/min, VM = 75 dm³/min, VH = 15 dm³/min.

On the other hand, the highest COP = 0.65 may be obtained for T_{Lin} = 291 K, T_{Min} = 298 K, T_{Hin} = 353 K, VL = 20 dm³/min, VM = 75 dm³/min, VH = 15 dm³/min.

4. Conclusions

The paper deals with one of the most effective cooling productions via an adsorption chiller, utilizing waste low-temperature and operating in an existing combined heating and cooling system. A two-bed AdC is considered in the study. Artificial neural networks are used to develop a unique, non-iterative ACANN model, allowing conducting the performance optimization study of the chiller. For the considered range of input parameters of the adsorption chiller, the highest CC equal to 12.7 kW can be obtained for T_{Lin} = 293 K, T_{Min} = 298 K, T_{Hin} = 353 K, VL = 20 dm³/min, VM = 75 dm³/min, VH = 15 dm³/min.

The highest COP = 0.65 can be obtained for the ice water input temperature T_{Lin} = 291 K, the recooling water inlet temperature T_{Min} = K, the hot water inlet temperature, T_{Hin} = 353 K, the ice water volume flow rate, VL = 20 dm³/min, the recooling water volume flow rate VM = 75 dm³/min, the hot water volume flow rate VH = 0.15 dm³/min.

The developed ACANN model constitutes an easy-to-use and powerful optimization tool of the adsorption chiller, integrated into a combined, multigeneration system.

Acknowledgements. Scientific work was performed within Project No. 2018/29/B/ST8/00442, “Research on sorption processes intensification methods in modified construction of adsorbent beds,” supported by National Science Center, Poland. The support is gratefully acknowledged. The authors express their thanks to KEZO Research Centre, Polish Academy of Sciences, ul. Akademijna 27, 05-110 Jablonna, Poland, for access allowing conducting the experiments.

REFERENCES

- [1] S. Moser and S. Lassacher, “External use of industrial waste heat – An analysis of existing implementations in Austria”, *J. Clean Prod.* 264, 121531 (2020).
- [2] J. Krzywanski, K. Grabowska, F. Herman, P. Pyrka, M. Sosnowski, T. Prauzner, and W. Nowak, “Optimization of a three-bed adsorption chiller by genetic algorithms and neural networks”, *Energy Conv. Manag.* 153, 313–322 (2017).
- [3] B. Rezaie and M.A. Rosen, “District heating and cooling: Review of technology and potential enhancements”, *Appl. Energy* 93, 2–10 (2012).
- [4] A.P. Roskilly and M. Ahmad Al-Nimr, “Sustainable Thermal Energy Management”, *Energy Conv. Manag.* 159, 396–397 (2018).
- [5] H. Lund, S. Werner, R. Wiltshire, S. Svendsen, J.E. Thorsen, F. Hvelplund, and B.V. Mathiesen, “4th Generation District Heating (4GDH): Integrating smart thermal grids into future sustainable energy systems”, *Energy* 68, 1–11 (2014).
- [6] M. Widziński, P. Chaja, A. Andersen, M. Jaroszewska, S. Bykuć, and J. Sawicki, “Simulation of an alternative energy system for district heating company in the light of changes in regulations of the emission of harmful substances into the atmosphere”, *Int. J. Sustain. Energy Plan. Manag.* 24, 43–56 (2019).
- [7] M. Chorowski and P. Pyrka, “Modelling and experimental investigation of an adsorption chiller using low-temperature heat from cogeneration”, *Energy* 92, 221–229 (2015).
- [8] R. AL-Dadah, S. Mahmoud, E. Elsayed, P. Youssef, and F. Al-Mousawi, “Metal-organic framework materials for adsorption heat pumps”, *Energy* 190, 116356 (2020).
- [9] M. Sosnowski, “Evaluation of Heat Transfer Performance of a Multi-Disc Sorption Bed Dedicated for Adsorption Cooling Technology”, *Energies* 12, 4660 (2019).
- [10] A.S. Alsaman, A.A. Askalany, K. Harby, and M.S. Ahmed, “Performance evaluation of a solar-driven adsorption desalination-cooling system”, *Energy* 128, 196–207 (2017).
- [11] A. Kulakowska, A. Pajdak, J. Krzywanski, K. Grabowska, A. Zylka, M. Sosnowski, M. Wesolowska, K. Sztেকler, and W. Nowak, “Effect of Metal and Carbon Nanotube Additives on the Thermal Diffusivity of a Silica Gel-Based Adsorption Bed”, *Energies* 13, 1391 (2020).

- [12] J. Ling-Chin, H. Bao, Z. Ma, W. Taylor, and A. Paul Roskilly, “State-of-the-Art Technologies on Low-Grade Heat Recovery and Utilization in Industry”, in *Energy Conversion – Current Technologies and Future Trends*, eds. I.H. Al-Bahadly, IntechOpen, 2019.
- [13] K. Grabowska, J. Krzywanski, W. Nowak, and M. Wesolowska, “Construction of an innovative adsorbent bed configuration in the adsorption chiller – Selection criteria for effective sorbent-glue pair”, *Energy* 151, 317–323 (2018).
- [14] K. Grabowska, M. Sosnowski, J. Krzywanski, K. Sztékler, W. Kalawa, A. Zylka, and W. Nowak, “The Numerical Comparison of Heat Transfer in a Coated and Fixed Bed of an Adsorption Chiller”, *J. Therm. Sci.* 27, 421–426 (2018).
- [15] I.H. Al-Bahadly, *Energy Conversion – Current Technologies and Future Trends*, London, 2019.
- [16] J. Krzywanski, K. Grabowska, M. Sosnowski, A. Zylka, K. Sztékler, W. Kalawa, T. Wójcik, and W. Nowak, “An Adaptive Neuro-Fuzzy model of a Re-Heat Two-Stage Adsorption Chiller”, *Therm. Sci.* 23, 1053–1063 (2019).
- [17] K.J. Chua, S.K. Chou, W.M. Yang, and J. Yan, “Achieving better energy-efficient air conditioning – A review of technologies and strategies”, *Appl. Energy* 104, 87–104 (2013).
- [18] X.H. Li, X.H. Hou, X. Zhang, and Z.X. Yuan, “A review on development of adsorption cooling—Novel beds and advanced cycles”, *Energy Conv. Manag.* 94, 221–232 (2015).
- [19] K. Sztékler, W. Kalawa, Ł. Mika, J. Krzywanski, K. Grabowska, M. Sosnowski, W. Nowak, T. Siwek, and A. Bieniek, “Modeling of a Combined Cycle Gas Turbine Integrated with an Adsorption Chiller”, *Energies* 13, 515 (2020).
- [20] Y.I. Aristov, I.S. Glaznev, and I.S. Girmik, “Optimization of adsorption dynamics in adsorptive chillers: Loose grains configuration”, *Energy* 46, 484–492 (2012).
- [21] I.S. Girmik, A.D. Grekova, L.G. Gordeeva, and Yu.I. Aristov, “Dynamic optimization of adsorptive chillers: Compact layer vs. bed of loose grains”, *Appl. Therm. Eng.* 125, 823–829 (2017).
- [22] U. Bau, N. Baumgärtner, J. Seiler, F. Lanzerath, C. Kirches, and A. Bardow, “Optimal operation of adsorption chillers: First implementation and experimental evaluation of a nonlinear model-predictive-control strategy”, *Appl. Therm. Eng.* 149, 1503–1521 (2019).
- [23] M.B. Elsheniti, M.A. Hassab, and A.-E. Attia, “Examination of effects of operating and geometric parameters on the performance of a two-bed adsorption chiller”, *Appl. Therm. Eng.* 146, 674–687 (2019).
- [24] J. Krzywanski, K. Grabowska, M. Sosnowski, A. Żyłka, K. Sztékler, W. Kalawa, T. Wójcik, and W. Nowak, “Modeling of a re-heat two-stage adsorption chiller by AI approach”, *MATEC Web Conf.* 240, 1–3 (2018).
- [25] S. Narayanan, S. Yang, H. Kim, and E.N. Wang, “Optimization of adsorption processes for climate control and thermal energy storage”, *Int. J. Heat Mass Transf.* 77, 288–300 (2014).
- [26] I.I. El-Sharkawy, H. AbdelMeguid, and B.B. Saha, “Towards an optimal performance of adsorption chillers: Reallocation of adsorption/desorption cycle times”, *Int. J. Heat Mass Transf.* 63, 171–182 (2013).
- [27] Q.W. Pan, R.Z. Wang, and L.W. Wang, “Comparison of different kinds of heat recoveries applied in adsorption refrigeration system”, *Int. J. Refrig.* 55, 37–48 (2015).
- [28] R.P. Sah, B. Choudhury, R.K. Das, and A. Sur, “An overview of modelling techniques employed for performance simulation of low-grade heat operated adsorption cooling systems”, *Renew. Sust. Energ. Rev.* 74, 364–376 (2017).
- [29] L. Rutkowski, *Computational Intelligence: Methods and Techniques*, Springer Science & Business Media (2008).
- [30] J. Szczepański, J. Klamka, K.M. Węgrzyn-Wolska, I. Rojek, and P. Prokopowicz, “Computational Intelligence and Optimization Techniques in Communications and Control”, *Bull. Pol. Acad. Sci. Tech. Sci.* 68(2), 181–184 (2020).
- [31] B. Paprocki, A. PREGOWSKA, and J. Szczepanski, “Optimizing information processing in brain-inspired neural networks”, *Bull. Pol. Acad. Sci. Tech. Sci.* 68(2), 225–233 (2020).
- [32] A. Cichocki, T. Poggio, S. Osowski, and V. Lempitsky, “Deep Learning: Theory and Practice”, *Bull. Pol. Acad. Sci. Tech. Sci.* 66(6), 757–759 (2018).
- [33] T. Poggio and Q. Liao, “Theory I: Deep networks and the curse of dimensionality”, *Bull. Pol. Acad. Sci. Tech. Sci.* 66(6), 761–773 (2018).
- [34] T. Poggio and Q. Liao, “Theory II: Deep learning and optimization”, *Bull. Pol. Acad. Sci. Tech. Sci.* 66(6), 775–787 (2018).
- [35] M. Figurnov, A. Sobolev, and D. Vetrov, “Probabilistic adaptive computation time”, *Bull. Pol. Acad. Sci. Tech. Sci.* 66(6), 811–820 (2018).
- [36] V. Lebedev and V. Lempitsky, “Speeding-up convolutional neural networks: A survey”, *Bull. Pol. Acad. Sci. Tech. Sci.* 66(6), 799–810 (2018).
- [37] S.C. Cagan, M. Aci, B.B. Buldum, and C. Aci, “Artificial neural networks in mechanical surface enhancement technique for the prediction of surface roughness and microhardness of magnesium alloy”, *Bull. Pol. Acad. Sci. Tech. Sci.* 67(4), 729–739 (2019).
- [38] I. Rojek and E. Dostatni, “Machine learning methods for optimal compatibility of materials in ecodesign”, *Bull. Pol. Acad. Sci. Tech. Sci.* 68(2), 199–206 (2020).
- [39] S. Osowski and K. Siwek, “Local dynamic integration of ensemble in prediction of time series”, *Bull. Pol. Acad. Sci. Tech. Sci.* 67(3), 517–525 (2019).
- [40] J. Kurek, B. Świdorski, S. Osowski, M. Kruk, and W. Barhoumi, “Deep learning versus classical neural approach to mammogram recognition”, *Bull. Pol. Acad. Sci. Tech. Sci.* 66(6), 831–840 (2018).
- [41] Q. Zhao, Y. Qiu, G. Zhou, and A. Cichocki, “Comparative study on the classification methods for breast cancer diagnosis”, *Bull. Pol. Acad. Sci. Tech. Sci.* 66(6), 841–848 (2018).
- [42] V. Osin, A. Cichocki, and E. Burnaev, “Fast multispectral deep fusion networks”, *Bull. Pol. Acad. Sci. Tech. Sci.* 66(6), 875–889 (2018).
- [43] J. Jakubowski and J. Chmielińska, “Detection of driver fatigue symptoms using transfer learning”, *Bull. Pol. Acad. Sci. Tech. Sci.* 66(6), 869–874 (2018).
- [44] P. Prokopowicz, D. Mikołajewski, K. Tyburek, and E. Mikołajewska, “Computational gait analysis for post-stroke rehabilitation purposes using fuzzy numbers, fractal dimension and neural networks”, *Bull. Pol. Acad. Sci. Tech. Sci.* 68(2), 191–198 (2020).
- [45] B. Cieniawska, K. Pentoś, and D. Łuczycka, “Neural modeling and optimization of the coverage of the sprayed surface”, *Bull. Pol. Acad. Sci. Tech. Sci.* 68(3), 601–608 (2020).
- [46] Y. Li, B. Zhang, and X. Xu, “Decoupling control for permanent magnet in-wheel motor using internal model control based on back-propagation neural network inverse system”, *Bulletin of the Polish Academy of Sciences: Technical Science* 66(6), 961–972 (2018).
- [47] R. Korupczyński and J. Trajer, “Assessment of wind energy resources using artificial neural networks – case study at Łódź Hills”, *Bull. Pol. Acad. Sci. Tech. Sci.* 67, 115–124 (2019).

- [48] J. Krzywanski, H. Fan, Y. Feng, A.R. Shaikh, M. Fang, and Q. Wang, "Genetic algorithms and neural networks in optimization of sorbent enhanced H₂ production in FB and CFB gasifiers", *Energy Conv. Manag.* 171, 1651–1661 (2018).
- [49] J. Krzywanski, M. Wesolowska, A. Blaszczyk, A. Majchrzak, M. Komorowski, and W. Nowak, "The Non-Iterative Estimation of Bed-to-Wall Heat Transfer Coefficient in a CFBC by Fuzzy Logic Methods", *Procedia Eng.* 157, 66–71 (2016).
- [50] W. Muskała, J. Krzywański, R. Rajczyk, M. Cecerko, B. Kierzkowski, W. Nowak, and W. Gajewski, "Investigation of erosion in CFB boilers", *Rynek Energii* 87, 97–102 (2010).
- [51] W. Muskała, J. Krzywański, R. Sekret, and W. Nowak, "Model research of coal combustion in circulating fluidized bed boilers" *Chem. Process Eng.* 29, 473–492 (2008).
- [52] A. Zylka, J. Krzywanski, T. Czakiert, K. Idziak, M. Sosnowski, K. Grabowska, T. Prauzner, and W. Nowak, "The 4th Generation of CeSFaMB in numerical simulations for CuO-based oxygen carrier in CLC system", *Fuel* 255, 115776 (2019).
- [53] A. Blaszczyk and J. Krzywański, "A comparison of fuzzy logic and cluster renewal approaches for heat transfer modeling in a 1296 t/h CFB boiler with low level of flue gas recirculation", *Arch. Thermodyn.* 38, 91–122 (2017).
- [54] J. Krzywanski, M. Wesolowska, A. Blaszczyk, A. Majchrzak, M. Komorowski, and W. Nowak, "Fuzzy logic and bed-to-wall heat transfer in a large-scale CFBC", *Nt. J. Numer. Methods Heat Fluid Flow* 28, 254–266 (2018).
- [55] Machine learning software, Neural Designer. [Online] <https://www.neuraldesigner.com/> (accessed on Jun 11, 2019).
- [56] J. Krzywanski, A. Blaszczyk, T. Czakiert, R. Rajczyk, and W. Nowak, "Artificial intelligence treatment of NO_x emissions from CFBC in air and oxy-fuel conditions", *CFB-11: Proceedings of the 11th International Conference on Fluidized Bed Technology*, 2014, pp. 619–624.
- [57] J. Krzywański and W. Nowak, "Neurocomputing approach for the prediction of NO_x emissions from CFBC in air-fired and oxygen-enriched atmospheres", *J. Power Technol.* 97, 75–84 (2017).
- [58] Z. Salam, J. Ahmed, and B.S. Merugu, "The application of soft computing methods for MPPT of PV system: A technological and status review", *Appl. Energy* 107, 135–148 (2013).
- [59] J. Krzywanski, "A General Approach in Optimization of Heat Exchangers by Bio-Inspired Artificial Intelligence Methods", *Energies* 12, 4441 (2019).
- [60] J. Krzywanski and W. Nowak, "Modeling of heat transfer coefficient in the furnace of CFB boilers by artificial neural network approach", *Int. J. Heat Mass Transf.* 55, 4246–4253 (2012).
- [61] J. Krzywanski and W. Nowak, "Modeling of bed-to-wall heat transfer coefficient in a large-scale CFBC by fuzzy logic approach", *Int. J. Heat Mass Transf.* 94, 327–334 (2016).
- [62] A.K. Kar, "Bio inspired computing – A review of algorithms and scope of applications", *Expert Syst. Appl.* 59, 20–32 (2016).
- [63] C.Y. Tso, C.Y.H. Chao, and S.C. Fu, "Performance analysis of a waste heat driven activated carbon based composite adsorbent – Water adsorption chiller using simulation model", *Int. J. Heat Mass Transf.* 55, 7596–7610 (2012).
- [64] L. Yang and W. Wang, "The heat transfer performance of horizontal tube bundles in large falling film evaporators", *Int. J. Refrig.* 34, 303–316 (2011).
- [65] W. Kalawa, K. Grabowska, K. Sztekler, J. Krzywański, M. Sosnowski, S. Stefański, T. Siwek, and W. Nowak, "Progress in design of adsorption refrigeration systems. Evaporators", *EPJ Web Conf.* 213, 02035 (2019).
- [66] B.B. Saha, S. Koyama, J.B. Lee, K. Kuwahara, K.C.A. Alam, Y. Hamamoto, A. Akisawa, and T. Kashiwagi, "Performance evaluation of a low-temperature waste heat driven multi-bed adsorption chiller", *Int. J. Multiph. Flow* 29, 1249–1263 (2003).
- [67] J. Jeon, S. Lee, D. Hong, and Y. Kim, "Performance evaluation and modeling of a hybrid cooling system combining a screw water chiller with a ground source heat pump in a building", *Energy* 35, 2006–2012 (2010).
- [68] B.B. Saha, E.C. Boelman, and T. Kashiwagi, "Computer simulation of a silica gel-water adsorption refrigeration cycle – the influence of operating conditions on cooling output and COP", *ASHRAE Trans.: Res.* 101, 348–357 (1995).
- [69] K. Habib, B.B. Saha, A. Chakraborty, S. Koyama, and K. Srinivasan, "Performance evaluation of combined adsorption refrigeration cycles", *Int. J. Refrig.* 34, 129–137 (2011).
- [70] B.B. Saha, S. Koyama, T. Kashiwagi, A. Akisawa, K.C. Ng, and H.T. Chua, "Waste heat driven dual-mode, multi-stage, multi-bed regenerative adsorption system", *Int. J. Refrig.* 26, 749–757 (2003).
- [71] A. Li, A.B. Ismail, K. Thu, K.C. Ng, and W.S. Loh, "Performance evaluation of a zeolite–water adsorption chiller with entropy analysis of thermodynamic insight", *Appl. Energy* 130, 702–711 (2014).